The IRM
Quarterly
Summer 2014, Vol. 24 No.2
ISSN: 2152-1972

Inside...

The iron that binds: The unexpectedly strong magnetism of high-temperature ceramic cements commonly used in rock magnetic experiments.

Evgeniya Khakhalova and Josh M. Feinberg
IRM

The main goal of many IRM visitors is to better understand the composition of the magnetic remanence carriers in their samples. Typically, a material's Curie or Néel temperature serves as the primary means for estimating its mineralogical composition. However, many of the most commonly used techniques, such as high temperature susceptibility and thermal demagnetization experiments, have to be interpreted carefully due to the complicating effects of grain size. For example, single-domain grains contribute less signal to susceptibility experiments than superparamagnetic and multidomain grains of the same material, and thermal demagnetization experiments are insensitive to superparamagnetic grains. Further, the unblocking temperatures observed in a thermal demagnetization experiment will typically be lower than the Curie or Néel temperature of the material.

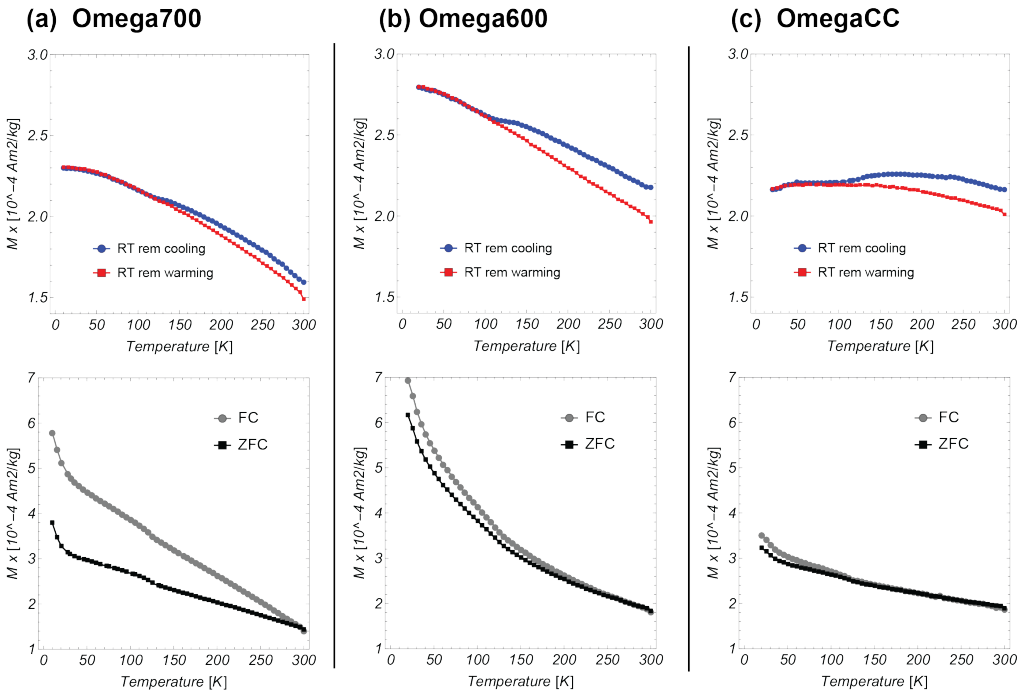

Fig 1. RT SIRM curves on cooling from 300 K to 10 K and warming from 10 K to 300 K and SIRM warming curves from 10 K to 300 K after field-cooling (FC) and zero-field-cooling (ZFC) of samples (a) Omega700_3, (b) Omega600, and (c) OmegaCC. SIRM was imparted using a field of 2.5 T.

In this context, strong-field thermomagnetic experiments are the only technique in our magnetic toolkit that provides an unfettered view of the composition of a magnetic material. These experiments involve the measurement of a specimen's induced magnetization in the presence of a high field (1-2.5 T) across a range of elevated temperatures, often up to 700°C. Typically these experiments are conducted using a vibrating sample magnetometer (VSM) and require the use of a high temperature cement. The magnetic qualities of this high temperature cement have become increasingly important as more and more of our IRM visitors are examining samples with exceedingly low concentrations of magnetic material (e.g., silicate-hosted magnetic inclusions) or samples with very weak induced moments (e.g., samples dominated by hematite, goethite, and ferrihydrite). In these instances, any source of magnetic contamination in a strong-field thermomagnetic experiment can lead to an incorrect interpretation of a sample's magnetic mineralogy.

Here we examine the magnetic properties of some of the most commonly used high temperature cement. We present data for three types of Omega High Temperature cement. While these cements are ideal for highly magnetic geological materials, including most igneous rock types, the magnetism of these cements can be surprisingly high and on par with more weakly magnetized natural materials, and so we present this IRM Quarterly article as a kind of cautionary tale to the uninitiated.

What are high temperature ceramic cements made of?

In many ways high temperature ceramic cements are ideal for rock magnetic applications. They are stable across an enormous range of temperatures (from -200°C

cont'd. on pg. 9...

Visiting Fellows' Reports

Rock magnetic characterization of Cretaceous/Paleogene fluvial deposits from the Hell Creek Region, MT: A search for titanohematite

Courteny J. Sprain
Department of Earth and Planetary Science
University of California-Berkeley
spra0111@berkeley.edu

Despite decades of intense study, the relative significance of potential causes of the Cretaceous-Paleogene mass extinction, such as voluminous (>106 km^3) volcanic eruptions of the Deccan Traps and the large impact recorded by the Chicxulub crater, remains in debate (Schulte et al., 2010; Archibald et al., 2010; Courtillot et al., 2010; Keller et al., 2010). Testing different extinction hypotheses is inhibited by insufficient geochronology, exemplified in the geomagnetic polarity timescale (GPTS). The GPTS is used for age control in numerous KPB studies that lack means for direct dating, ranging from the investigation of climate change to evolution of life across the KPB. If well-calibrated with high precision ages, the GPTS would provide a powerful tool for probing deeper into the events surrounding the mass extinction.

Terrestrial fluvial deposits that make up the Hell Creek and Tullock Formations within the Hell Creek region of NE Montana (USA) provide an opportunity to refine the ages of polarity reversals near the KPB (C30n-C28n). Interbedded in these formations are abundant sanidine (K-feldspar) bearing ashes, which have yielded 40Ar/39Ar ages with resolution as good as ± 11 ka and absolute accuracy in the range of ± 40 ka (Renne et al, 2013; Sprain et al., 2014). By tying high-precision 40Ar/39Ar ages to reversals in a magnetostratigraphic study we can obtain ages for circum-KPB chron boundaries at an unprecedented precision, facilitating the comparison of KPB studies worldwide and enhancing our understanding of the causes and timing of the circum-KPB ecological crises and recovery.

To further add confidence to our magnetostratigraphic results, I conducted rock magnetic analyses at the Institute for Rock Magnetism focusing on the characterization of magnetic mineralogy and grain size distribution of magnetic minerals. Previous paleomagnetic work in the Hell Creek region conducted during the early 1980's and 1990's used strong-field thermomagnetic analysis, X-ray diffraction, and electron microprobe analysis to determine magnetic mineralogy. The results of these studies indicated that the dominant ferromagnetic mineral was intermediate-composition titanohematite, with a Curie temperature between 160–300°C (Swisher et al., 1993). These results are similar to those observed for other KPg Laramide continental deposits in the San Juan Basin, New Mexico and within the Williston Basin, North Dakota (Butler & Lindsay, 1985; Lund et al., 2002). No further rock magnetic analyses have been conducted on rocks from the Hell Creek region since Swisher et al. (1993). As such, my goal at the IRM was to update the magnetic characterization of our samples using modern equipment and techniques, and to test previous results, in particular the presence of titanohematite as the primary magnetic carrier of DRM in our samples.

High-temperature susceptibility experiments using the KappaBridge were conducted on a subset of samples comprising both whole rocks and magnetic extracts. Determination of Curie temperatures was unsuccessful for whole rock samples. For these samples, temperature curves were not reversible between heating and cooling, which was likely caused by the alteration of clay minerals to form magnetite during heating suggested by a susceptibility increase upon cooling. High temperature susceptibility experiments on magnetic extracts were much more successful. These experiments indicate that our samples have Curie temperatures that range from ~180°C to 300°C. This result is consistent with previous studies, and is in the range of expected Curie temperatures for intermediate composition titanohematite, although is not definitive proof as other phases such as titanomagnetite could also produce similar values.

To further constrain magnetic mineralogy, I conducted low-temperature experiments, including RTSIRM and FC/ZFC, using the "Old Blue" MPMS on whole rock samples and magnetic extracts. These experiments revealed that for a majority of samples the Verwey transition is present, although significantly suppressed, suggesting that a form of magnetite exists in our samples. RTSIRM curves show a significant increase in intensity towards lower temperatures, reminiscent of goethite (Fig.1). The heating RTSIRM curves remains below the cooling RTSIRM curves for most of our samples, which is likely due the presence of magnetite and cooling through the Verwey transition. Although RTSIRM curves suggest the presence of goethite, one of goethite's diagnostic features, a wide spread between FC and ZFC remanences, is not present in our samples. On the contrary, there is barely any spread between FC and ZFC curves at all (Fig. 1). A potential explanation for this observed trend is that the increased intensity towards lower temperatures in RTSIRM curves could be caused by the presence of intermediate-composition titanohematite, not goethite, as it also has a low ordering temperature (~200°C).

As a final check to see whether titanohematite is the primary magnetic carrier in our samples, I conducted a self-reversal test. Intermediate composition titanohematite has a unique property in that exsolved bands of Ti-rich and Ti-poor lamellae can interact such that the acquired remanence is recorded antiparallel to the applied field. To test for this property we imparted a TRM using a 100 μT field, at a max T of 300°C, for a soak time of 30 minutes. This

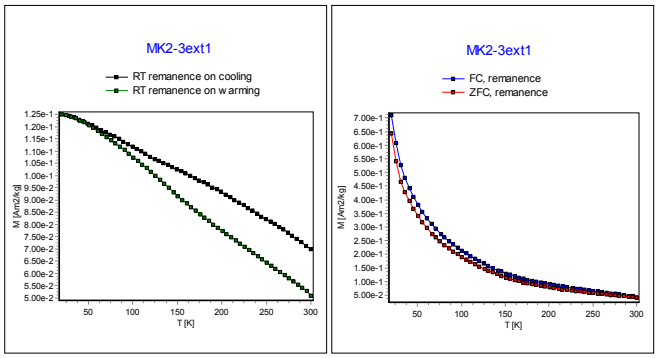

Fig 1. Low temperature experiments conducted on a magnetic extract from a siltstone within the Tullock Fm. The first panel shows measurements of magnetization during cooling and then warming following a SIRM applied at room temperature. The second panel shows measurements of magnetization during warming following a sustained DC field of 2.5 T during cooling (Field-cooled, FC), and measurements of magnetization during warming following a SIRM imparted at low temperature (Zero field-cooled, ZFC).

test was conducted on two samples. For the first sample the results were ambiguous. For the second sample, initial measurements showed a component of magnetization parallel to the applied field. Upon AF demagnetization, gradually up to 120 mT, a second component of magnetization became clear, exactly antiparallel to the applied field (Fig. 2). What this result shows is at least some of our samples have intermediate-composition titanohematite as a primary carrier of magnetization, but an additional component also exists, which due to the presence of a subdued Verwey transition and blocking temperatures below 300°C, is likely a form of non-stoichiometric magnetite, or maghemite. To confirm these results, I would like to conduct the self-reversal test on more samples, in addition to further characterizing magnetic mineralogy using X-ray diffraction. More work is needed to determine the grain size distribution of magnetic minerals in our samples, as the presence of titanohematite precludes the use of magnetic grain size indicators that are based on the assumption that magnetite is the dominant magnetic carrier.

I'd like to thank everyone at the IRM for their staunch support and kindness during my brief visit. In particular I'd like to thank Mike Jackson for showing me the ropes and being a great mentor through the whole process. In addition I'd like to thank Josh Feinberg for great intellectual support, and Bruce Moskowitz, who brilliantly suggested we try a self-reversal test.

References

Archibald, et al., 2010, Cretaceous extinctions: multiple causes: Science, v. 328, p. 973, author reply p. 975.

Butler, R.F., and Lindsay, E.H., 1985, Mineralogy of magnetic minerals and revised magnetic polarity stratigraphy of continental sediments, San-Juan Basin, New Mexico: Journal of Geology, v. 93, p. 535–554.

Courtillot, V. and Fluteau, F., 2010, Cretaceous Extinctions: The Volcanic Hypothesis: Science, v. 328, p. 973-974, author reply p. 975.

Keller, G., Adatte, T., Pardo, A., Bajpai, S., Khosla, A., and Samant, B., 2010, Cretaceous Extinctions: Evidence Overlooked: Science, v. 328, p. 974-975, author reply p. 975.

Lund, S.P., Hartman, J.H., and Banerjee, S.K., 2002, Magnetostratigraphy of interfingering upper Cretaceous–Paleocene marine and continental strata of the Williston Basin, North Dakota and Montana, in Hartman, J.H., Johnson, K.R., and Nichols, D.J., eds., The Hell Creek Formation and the Cretaceous-Tertiary boundary in the northern Great Plains: An integrated continental record of the end of the Cretaceous: Boulder, Colorado, Geological Society of America Special Paper 361, p. 57–74.

Renne, P.R., Deino, A.L., Hilgen, F.J., Kuiper, K.F., Mark, D.F., Mitchell, W.S., III, Morgan, L.E., Mundil, R., and Smit, J., 2013, Time Scales of critical events around the Cretaceous-Paleogene boundary: Science, v. 339, p. 684–687.

Schulte, P., et al., 2010, The Chicxulub asteroid impact and mass extinction at the Cretaceous-Paleogene boundary: Science, v. 327, p. 1214–1218.

Sprain, C. J., Renne, P.R., Wilson, G. P., and Clemens, W. A., 2014, High-Resolution Chronostratigraphy of the Terrestrial Cretaceous-Paleogene Transition and Recovery Interval in the Hell Creek Region, Montana: GSA Bulletin, doi: 10.1130/B31076.1

Swisher, C.C., III, Dingus, L., and Butler, R.F., 1993, 40Ar/39Ar dating and magnetostratigraphic correlation of the terrestrial Cretaceous-Paleogene boundary and Puercan Mammal Age, Hell Creek–Tullock formations, eastern Montana: Canadian Journal of Earth Sciences, v. 30, p. 1981–1995.

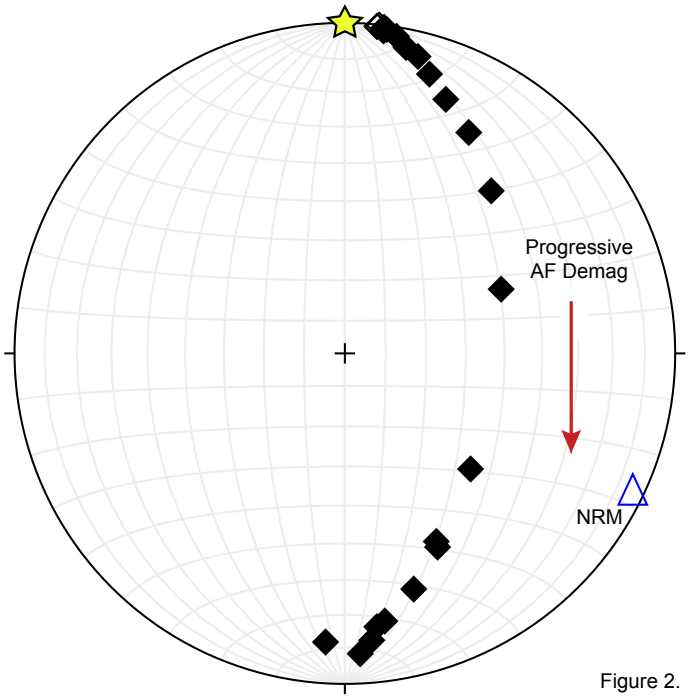

Figure 2.

Fig 2. Results of self-reversal test. Star indicates direction of applied field. Triangle shows initial NRM of specimen. Arrow points in the direction of increasing AF demagnetization.

Current Articles

A list of current research articles dealing with various topics in the physics and chemistry of magnetism is a regular feature of the IRM Quarterly. Articles published in familiar geology and geophysics journals are included; special emphasis is given to current articles from physics, chemistry, and materials-science journals. Most are taken from ISI Web of Knowledge, after which they are subjected to Procrustean culling for this newsletter. An extensive reference list of articles (primarily about rock magnetism, the physics and chemistry of magnetism, and some paleomagnetism) is continually updated at the IRM. This list, with more than 10,000 references, is available free of charge. Your contributions both to the list and to the Current Articles section of the IRM Quarterly are always welcome.

Archeomagnetism

Garcia, J., K. Martinez, G. Cuenca-Bescos, and E. Carbonell (2014), Human occupation of Iberia prior to the Jaramillo magnetochron (> 1.07 Myr), Quaternary Science Reviews, 98, 84-99.

Frahm, E., J. M. Feinberg, B. A. Schmidt-Magee, K. Wilkinson, B. Gasparyan, B. Yeritsyan, S. Karapetian, K. Meliksetian, M. J. Muth, and D. S. Adler (2014), Sourcing geochemically identical obsidian: multiscalar magnetic variations in the Gutansar volcanic complex and implications for Palaeolithic research in Armenia, Journal of Archaeological Science, 47, 164-178.

Lebatard, A. E., et al. (2014), Dating the Homo erectus bearing travertine from Kocabas (Denizli, Turkey) at at least 1.1 Ma, Earth and Planetary Science Letters, 390, 8-18.

Bio- Geomagnetism

Kornig, A., M. A. Hartmann, C. Teichert, P. Fratzl, and D. Faivre (2014), Magnetic force imaging of a chain of biogenic magnetite and Monte Carlo analysis of tip-particle interaction, Journal of Physics D-Applied Physics, 47(23).

Lin, T. J., E. A. Breves, M. D. Dyar, H. C. V. Eecke, J. W. Jamieson, and J. F. Holden (2014), Magnetite formation from ferrihydrite by hyperthermophilic archaea from Endeavour Segment, Juan de Fuca Ridge hydrothermal vent chimneys, Geobiology, 12(3), 200-211.

Paterson, G. A., Y. Z. Wang, and Y. X. Pan (2014), The fidelity of paleomagnetic records carried by magnetosome chains (vol 383, pg 82, 2013), Earth and Planetary Science Letters, 391, 159-159.

Environmental magnetism and Climate

Ahmed, E., and S. J. M. Holmstrom (2014), The effect of soil horizon and mineral type on the distribution of siderophores in soil, Geochimica Et Cosmochimica Acta, 131, 184-195.

Alexander, E. B. (2014), Arid to humid serpentine soils, mineralogy, and vegetation across the Klamath Mountains, USA, Catena, 116, 114-122.

Bellucci, L., F. Bona, P. Corrado, D. Magri, I. Mazzini, F. Parenti, G. Scardia, and R. Sardella (2014), Evidence of late Gelasian dispersal of African fauna at Coste San Giacomo (Anagni Basin, central Italy): Early Pleistocene environments and the background of early human occupation in Europe, Quaternary Science Reviews, 96, 72-85.

Bosboom, R. E., H. A. Abels, C. Hoorn, B. C. J. van den Berg, Z. Guo, and G. Dupont-Nivet (2014), Aridification in continental Asia after the Middle Eocene Climatic Optimum (MECO), Earth and Planetary Science Letters, 389, 34-42.

Bradak, B., and J. Kovacs (2014), Quaternary surface processes indicated by the magnetic fabric of undisturbed, reworked and fine-layered loess in Hungary, Quaternary International, 319, 76-87.

Buggle, B., U. Hambach, K. Muller, L. Zoller, S. B. Markovic, and B. Glaser (2014), Iron mineralogical proxies and Quaternary climate change in SE-European loess-paleosol sequences, Catena, 117, 4-22.

Carvalho, P. C. S., A. M. R. Neiva, M. Silva, and I. Antunes (2014), Metal and metalloid leaching from tailings into streamwater and sediments in the old Ag-Pb-Zn Terramonte mine, northern Portugal, Environmental Earth Sciences, 71(5), 2029-2041.

Chen, T., X. K. Qiang, H. Zhao, and Y. B. Sun (2014), An investigation of the magnetic carriers and demagnetization characteristics of the Gulang loess section, northwestern Chinese Loess Plateau, Geochemistry Geophysics Geosystems, 15(4), 1600-1616.

Clift, P. D., S. M. Wan, and J. Blusztajn (2014), Reconstructing chemical weathering, physical erosion and monsoon intensity since 25 Ma in the northern South China Sea: A review of competing proxies, Earth-Science Reviews, 130, 86-102.

Daigle, H., B. Thomas, H. Rowe, and M. Nieto (2014), Nuclear magnetic resonance characterization of shallow marine sediments from the Nankai Trough, Integrated Ocean Drilling Program Expedition 333, Journal of Geophysical Research-Solid Earth, 119(4), 2631-2650.

Djerrab, A., S. Spassov, N. Defaflia, J. Hus, S. Abdessadok, M. Ruault-Djerrab, N. Bahra, and S. Ech-Chakrouni (2014), The Middle Palaeolithic site of Birzgane (Tebessa, Algeria): Rock magnetic property characterisation and past rainfall reconstruction, Quaternary International, 320, 63-74.

Fitzsimmons, K. E., and U. Hambach (2014), Loess accumulation during the last glacial maximum: Evidence from Urluia, southeastern Romania, Quaternary International, 334, 74-85.

Gehring, A. U., N. Riahi, J. Kind, B. S. G. Almqvist, and P. G. Weidler (2014), The formation of the Namib Sand Sea inferred from the spatial pattern of magnetic rock fragments, Earth and Planetary Science Letters, 395, 168-172.

Geiss, C. E. (2014), Does timing or location matter? The influence of site variability and short-term variations in precipitation on magnetic enhancement in loessic soils, Geoderma, 230, 280-287.

Gocke, M., U. Hambach, E. Eckmeier, L. Schwark, L. Zoller, M. Fuchs, M. Loscher, and G. L. B. Wiesenberg (2014), Introducing an improved multiproxy approach for paleoenvironmental reconstruction of loess-paleosol archives applied on the Late Pleistocene Nussloch sequence (SW Germany), Palaeogeography Palaeoclimatology Palaeoecology, 410, 300-315.

Hosek, J., P. Pokorny, V. Kubovcik, I. Horacek, P. Zackova, J. Kadlec, F. Rojik, L. Lisa, and S. Buckuliakova (2014), Late glacial climatic and environmental changes in eastern-central Europe: Correlation of multiple biotic and abiotic proxies from the Lake Svarcenberk, Czech Republic, Palaeogeography Palaeoclimatology Palaeoecology, 396, 155-172.

Hu, X. F., Y. Du, C. L. Guan, Y. Xue, and G. L. Zhang (2014), Color variations of the Quaternary Red Clay in southern China and its paleoclimatic implications, Sedimentary Geology, 303, 15-+.

Kong, X. H., W. J. Zhou, J. W. Beck, F. Xian, and Z. K. Wu (2014), Asynchronous records of Brunhes/Matuyama reversal in marine sediments and Chinese loess: Review and discussion, Quaternary International, 319, 137-142.

Li, Y. L. (2014), Micro- and nanobands in late Archean and Palaeoproterozoic banded-iron formations as possible mineral records of annual and diurnal depositions, Earth and Planetary Science Letters, 391, 160-170.

Li, Z. J., D. H. Sun, F. H. Chen, F. Wang, Y. B. Zhang, F. Guo, X. Wang, and B. F. Li (2014), Chronology and paleoenvironmental records of a drill core in the central Tengger Desert of China, Quaternary Science Reviews, 85, 85-98.

Lise-Pronovost, A., G. St-Onge, C. Gogorza, G. Jouve, R. Francus, B. Zolitschka, and P. S. Team (2014), Rock-magnetic signature of precipitation and extreme runoff events in south-eastern Patagonia since 51,200 cal BP from the sediments of Laguna Potrok Aike, Quaternary Science Reviews, 98, 110-125.

Lukic, T., B. Basarin, B. Buggle, S. B. Markovic, V. M. Tomovic, J. P. Raljic, I. Hrnjak, A. Timar-Gabor, U. Hambach, and M. B. Gavrilov (2014), A joined rock magnetic and colorimetric perspective on the Late Pleistocene climate of Orlovat loess site (Northern Serbia), Quaternary International, 334, 179-188.

Lyons, R., S. Tooth, and G. A. T. Duller (2014), Late Quaternary climatic changes revealed by luminescence dating, mineral magnetism and diffuse reflectance spectroscopy of river terrace palaeosols: a new form of geoproxy data for the southern African interior, Quaternary Science Reviews, 95, 43-59.

Marques, J., D. S. Siqueira, L. A. Camargo, D. D. B. Teixeira, V. Barron, and J. Torrent (2014), Magnetic susceptibility and diffuse reflectance spectroscopy to characterize the spatial variability of soil properties in a Brazilian Haplustalf, Geoderma, 219, 63-71.

Marques, R., J. C. Waerenborgh, M. I. Prudencio, M. I. Dias, F. Rocha, and E. F. da Silva (2014), Iron speciation in volcanic topsoils from Fogo island (Cape Verde) - Iron oxide nanoparticles and trace elements concentrations, Catena, 113, 95-106.

Nie, J. S., R. Zhang, C. Necula, D. Heslop, Q. S. Liu, L. S. Gong, and S. Banerjee (2014), Late Miocene- early Pleistocene paleoclimate history of the Chinese Loess Plateau revealed by remanence unmixing, Geophysical Research Letters, 41(6), 2163-2168.

Perez, I., F. M. Romero, O. Zamora, and M. E. Gutierrez-Ruiz (2014), Magnetic susceptibility and electrical conductivity as a proxy for evaluating soil contaminated with arsenic, cadmium and lead in a metallurgical area in the San Luis Potosi State, Mexico, Environmental Earth Sciences, 72(5), 1521-1531.

Peterson, R. C., M. C. Williamson, and R. H. Rainbird (2014), Gossan Hill, Victoria Island, Northwest Territories: An analogue for mine waste reactions within permafrost and implication for the subsurface mineralogy of Mars, Earth and Planetary Science Letters, 400, 88-93.

Porsch, K., M. L. Rijal, T. Borch, L. D. Troyer, S. Behrens, F. Wehland, E. Appel, and A. Kappler (2014), Impact of organic carbon and iron bioavailability on the magnetic susceptibility of soils, Geochimica Et Cosmochimica Acta, 128, 44-57.

Prizomwala, S. P., N. Bhatt, and N. Basavaiah (2014), Understanding the sediment routing system along the Gulf of Kachchh coast, western India: Significance of small ephemeral rivers, Journal of Earth System Science, 123(1), 121-133.

Pufahl, P. K., S. L. Anderson, and E. E. Hiatt (2014), Dynamic sedimentation of Paleoproterozoic continental margin iron formation, Labrador Trough, Canada: Paleoenvironments and sequence stratigraphy, Sedimentary Geology, 309, 48-65.

Quijano, L., M. A. E. Chaparro, D. C. Marie, L. Gaspar, and A. Navas (2014), Relevant magnetic and soil parameters as potential indicators of soil conservation status of Mediterranean agroecosystems, Geophysical Journal International, 198(3), 1805-1817.

Razik, S., M. J. Dekkers, and T. von Dobeneck (2014), How environmental magnetism can enhance the interpretational value of grain-size analysis: A time-slice study on sediment export to the NW African margin in Heinrich Stadial 1 and Mid Holocene, Palaeogeography Palaeoclimatology Palaeoecology, 406, 33-48.

Saminpanya, S., J. Duangkrayom, P. Jintasakul, and R. Hanta (2014), Petrography, mineralogy and geochemistry of Cretaceous sediment samples from western Khorat Plateau, Thailand, and considerations on their provenance, Journal of Asian Earth Sciences, 83, 13-34.

Silva, J. D., S. Srinivasalu, P. D. Roy, and M. P. Jonathan (2014), Environmental conditions inferred from multi-element concentrations in sediments off Cauvery delta, Southeast India, Environmental Earth Sciences, 71(5), 2043-2058.

Song, Y. G., X. M. Fang, J. W. King, J. J. Li, I. Naoto, and Z. S. An (2014), Magnetic parameter variations in the Chaona loess/paleosol sequences in the central Chinese Loess Plateau, and their, significance for the middle Pleistocene climate transition, Quaternary Research, 81(3), 433-444.

Song, Y. G., X. L. Chen, L. B. Qian, C. X. Li, Y. Li, X. X. Li, H. Chang, and Z. S. An (2014), Distribution and composition of loess sediments in the Ili Basin, Central Asia, Quaternary International, 334, 61-73.

Song, Y., Q. Z. Hao, J. Y. Ge, D. A. Zhao, Y. Zhang, Q. Li, X. X. Zuo, Y. W. Lu, and P. Wang (2014), Quantitative relationships between magnetic enhancement of modern soils and climatic variables over the Chinese Loess Plateau, Quaternary International, 334, 119-131.

Thamo-Bozso, E., L. O. Kovacs, A. Magyari, and I. Marsi (2014), Tracing the origin of loess in Hungary with the help of heavy mineral composition data, Quaternary International, 319, 11-21.

Veerasingam, S., R. Venkatachalapathy, N. Basavaiah, T. Ramkumar, S. Venkatramanan, and K. Deenadayalan (2014), Identification and characterization of tsunami deposits off southeast coast of India from the 2004 Indian Ocean tsunami: Rock magnetic and geochemical approach, Journal of Earth System Science, 123(4), 905-921.

Villa, G., C. Fioroni, D. Persico, A. P. Roberts, and F. Florindo (2014), Middle Eocene to Late Oligocene Antarctic glaciation/deglaciation and Southern Ocean productivity, Paleoceanography, 29(3), 223-237.

Wang, X. S. (2014), Metal geochemical and mineral magnetic characterization of the < 2.5 mu m fraction of urban soils in Xuzhou (China), Environmental Earth Sciences, 71(8), 3491-3501.

Wang, X. S. (2014), Mineralogical and chemical composition of magnetic fly ash fraction, Environmental Earth Sciences, 71(4), 1673-1681.

Wang, S. Y., and S. G. Lu (2014), A rock magnetic study on red palaeosols in Yun-Gui Plateau (Southwestern China) and evidence for uplift of Plateau, Geophysical Journal International, 196(2), 736-747.

Yan, X. L., Y. F. Miao, J. B. Zan, W. L. Zhang, and S. Wu (2014), Late Cenozoic fluvial-lacustrine susceptibility increases in the Linxia Basin and their implications for Tibetan Plateau uplift, Quaternary International, 334, 132-140.

Zan, J. B., X. M. Fang, E. Appel, M. D. Yan, and S. L. Yang (2014), New insights into the magnetic variations of aeolian sands in the Tarim Basin and its paleoclimatic implications, Physics of the Earth and Planetary Interiors, 229, 82-87.

Zhang, G. L., and C. Smith-Duque (2014), Seafloor basalt alteration and chemical change in the ultra thinly sedimented South Pacific, Geochemistry Geophysics Geosystems, 15(7), 3066-3080.

Zhang, Y. B., D. H. Sun, Z. J. Li, F. Wang, X. Wang, B. F. Li, F. Guo, and S. Wu (2014), Cenozoic record of aeolian sediment accumulation and aridification from Lanzhou, China, driven by Tibetan Plateau uplift and global climate, Global and Planetary Change, 120, 1-15.

Zhao, J. B., J. J. Cao, Z. D. Jin, S. Xing, and T. J. Shao (2014), The fifth paleosol layer in the southern part of China's Loess Plateau and its environmental significance, Quaternary International, 334, 189-196.

Extraterrestiram and Planetary Magnetism

Arkani-Hamed, J., and D. Boutin (2014), Analysis of isolated magnetic anomalies and magnetic signatures of impact craters: Evidence for a core dynamo in the early history of the Moon, Icarus, 237, 262-277.

Redfern, G. van der Laan, and R. J. Harrison (2014), Nanopaleomagnetism of meteoritic Fe-Ni studied using X-ray photoemission electron microscopy, Earth and Planetary Science Letters, 396, 125-133.

Davidson, J., A. N. Krot, K. Nagashima, E. Hellebrand, and D. S. Lauretta (2014), Oxygen isotope and chemical compositions of magnetite and olivine in the anomalous CK3 Watson 002 and ungrouped Asuka-881595 carbonaceous chondrites: Effects of parent body metamorphism, Meteoritics & Planetary Science, 49(8), 1456-1474.

Fergason, R. L., L. R. Gaddis, and A. D. Rogers (2014), Hematite-bearing materials surrounding Candor Mensa in Candor Chasma, Mars: Implications for hematite origin and post-emplacement modification, Icarus, 237, 350-365.

Gattacceca, J., C. Suavet, P. Rochette, B. P. Weiss, M. Winklhofer, M. Uehara, and J. M. Friedrich (2014), Metal phases in ordinary chondrites: Magnetic hysteresis properties and implications for thermal history, Meteoritics & Planetary Science, 49(4), 652-676.

Gattacceca, J., P. Rochette, R. B. Scorzelli, P. Munayco, C. Agee, Y. Quesnel, C. Cournede, and J. Geissman (2014), Martian meteorites and Martian magnetic anomalies: A new perspective from NWA 7034, Geophysical Research Letters, 41(14), 4859-4864.

Harju, E. R., A. E. Rubin, I. Ahn, B. G. Choi, K. Ziegler, and J. T. Wasson (2014), Progressive aqueous alteration of CR carbonaceous chondrites, Geochimica Et Cosmochimica Acta, 139, 267-292.

Kohout, T., M. Gritsevich, V. I. Grokhovsky, G. A. Yakovlev, J. Haloda, P. Halodova, R. M. Michallik, A. Penttila, and K. Muinonen (2014), Mineralogy, reflectance spectra, and physical properties of the Chelyabinsk LL5 chondrite - Insight into shock-induced changes in asteroid regoliths, Icarus, 228, 78-85.

Laneuville, M., M. A. Wieczorek, D. Breuer, J. Aubert, G. Morard, and T. Ruckriemen (2014), A long-lived lunar dynamo powered by core crystallization, Earth and Planetary Science Letters, 401, 251-260.

Langlais, B., H. Amit, H. Larnier, E. Thebault, and A. Mocquet (2014), A new model for the (geo)magnetic power spectrum, with application to planetary dynamo radii, Earth and Planetary Science Letters, 401, 347-358.

Luecke, W., A. Kontny, and U. Kramar (2014), Geochemical zoning and magnetic mineralogy at Fe,Ni-alloy-troilite interfaces of three iron meteorites from Morasko, Coahuila II, and Mundrabilla, Meteoritics & Planetary Science, 49(5), 750-771.

Marrocchi, Y., M. Gounelle, I. Blanchard, F. Caste, and A. T. Kearsley (2014), The Paris CM chondrite: Secondary minerals and asteroidal processing, Meteoritics & Planetary Science, 49(7), 1232-1249.

Urrutia-Fucugauchi, J., L. Perez-Cruz, and D. Flores-Gutierrez (2014), Meteorite paleomagnetism - From magnetic domains to planetary fields and core dynamos, Geofisica Internacional, 53(3), 343-363.

Fundamental Rock and Mineral Magnetism

Brok, E., M. Sales, K. Lefmann, L. T. Kuhn, W. F. Schmidt, B. Roessli, P. Robinson, S. A. McEnroe, and R. J. Harrison (2014), Experimental evidence for lamellar magnetism in hemo-ilmenite by polarized neutron scattering, Physical Review B, 89(5).

Brown, L. L., J. Webber, M. Williams, S. Regan, and S. Seaman (2014), Magnetism of the lower crust: Observations from the Chipman Domain, Athabasca Granulite Terrain, northern Canada, Tectonophysics, 624, 66-74. Bryson, J. F. J., J. Herrero-Albillos, F. Kronast, M. Ghidini, S. A. T.

Clark, D. A. (2014), Magnetic effects of hydrothermal alteration in porphyry copper and iron-oxide copper-gold systems: A review, Tectonophysics, 624, 46-65.

Friedman, S. A., J. M. Feinberg, E. C. Ferre, F. Demory, F. Martin-Hernandez, J. A. Conder, and P. Rochette (2014), Craton vs. rift uppermost mantle contributions to magnetic anomalies in the United States interior, Tectonophysics, 624, 15-23.

Ge, K. P., W. Williams, Q. S. Liu, and Y. Yu (2014), Effects of the core-shell structure on the magnetic properties of partially oxidized magnetite grains: Experimental and micromagnetic investigations, Geochemistry Geophysics Geosystems, 15(5), 2021-2038.

Klein, F., W. Bach, S. E. Humphris, W. A. Kahl, N. Jons, B. Moskowitz, and T. S. Berquo (2014), Magnetite in seafloor serpentinite-Some like it hot, Geology, 42(2), 135-138.

Li, Z. Y., J. P. Zheng, Q. L. Zeng, Q. S. Liu, and W. L. Griffin (2014), Magnetic mineralogy of pyroxenite xenoliths from Hannuoba basalts, northern North China Craton: Implications for magnetism in the continental lower crust, Journal of Geophysical Research-Solid Earth, 119(2), 806-821.

Liu, D. L., H. B. Li, T. Q. Lee, Y. M. Chou, S. R. Song, Z. M. Sun, M. L. Chevalier, and J. L. Si (2014), Primary rock magnetism for the Wenchuan earthquake fault zone at Jiulong outcrop, Sichuan Province, China, Tectonophysics, 619, 58-69.

Maffione, M., A. Morris, O. Plumper, and D. J. J. van Hinsbergen (2014), Magnetic properties of variably serpentinized peridotites and their implication for the evolution of oceanic core complexes, Geochemistry Geophysics Geosystems, 15(4), 923-944.

Martin-Hernandez, F., E. C. Ferre, and S. A. Friedman (2014), Remanent magnetization in fresh xenoliths derived from combined demagnetization experiments: Magnetic mineralogy, origin and implications for mantle sources of magnetic anomalies, Tectonophysics, 624, 24-31.

McCollom, T. M., B. L. Ehlmann, A. Wang, B. M. Hynek, B. Moskowitz, and T. S. Berquo (2014), Detection of iron substitution in natroalunite-natrojarosite solid solutions and potential implications for Mars, American Mineralogist, 99(5-6), 948-964.

Miot, J., J. H. Li, K. Benzerara, M. T. Sougrati, G. Ona-Nguema, S. Bernard, J. C. Jumas, and F. Guyot (2014), Formation of single domain magnetite by green rust oxidation promoted by microbial anaerobic nitrate-dependent iron oxidation, Geochimica Et Cosmochimica Acta, 139, 327-343.

Ozdemir, O., and D. J. Dunlop (2014), Hysteresis and coercivity of hematite, Journal of Geophysical Research-Solid Earth, 119(4), 2582-2594.

Pei, J. L., H. B. Li, H. Wang, J. L. Si, Z. M. Sun, and Z. Z. Zhou (2014), Magnetic properties of the Wenchuan Earthquake Fault Scientific Drilling Project Hole-1 (WFSD-1), Sichuan Province, China, Earth Planets and Space, 66.

Robinson, P., F. Langenhorst, S. A. McEnroe, K. Fabian, and T. B. Ballaran (2014), Ferroan geikielite and coupled spinel-rutile exsolution from titanohematite: Interface characterization and magnetic properties, American Mineralogist, 99(8-9), 1694-1712.

Robinson, P., S. A. McEnroe, K. Fabian, R. J. Harrison, C. I. Thomas, and H. Mukai (2014), Chemical and magnetic properties of rapidly cooled metastable ferri-ilmenite solid solutions - IV: the fine structure of self-reversed thermoremanent magnetization, Geophysical Journal International, 196(3), 1375-1396.

Till, J. L., Y. Guyodo, F. Lagroix, G. Ona-Nguema, and J. Brest (2014), Magnetic comparison of abiogenic and biogenic alteration products of lepidocrocite, Earth and Planetary Science Letters, 395, 149-158.
Tuckova, M., R. Harman, P. Tucek, and J. Tucek (2014), Design of experiment for hysteresis loops measurement, Journal of Magnetism and Magnetic Materials, 368, 64-69.
Winklhofer, M., L. Chang, and S. H. K. Eder (2014), On the magnetocrystalline anisotropy of greigite (Fe3S4), Geochemistry Geophysics Geosystems, 15(4), 1558-1579.

Magnetic Fabrics and Anisotropy

Almqvist, B. S. G., B. Henry, M. J. Jackson, T. Werner, and F. Lagroix (2014), Methods and applications of magnetic anisotropy: A special issue in recognition of the career of Graham J. Borradaile, Tectonophysics, 629, 1-5.
Anchuela, O. P., A. G. Imaz, I. Gil-Pena, A. Maestro, J. Galindo-Zaldivar, J. Lopez-Martinez, J. Rey, R. Soto, and B. Oliva-Urcia (2014), Application of AMS for reconstruction of the geological evolution of recent volcanic systems: Case of Deception Island (South Shetland Islands, Antarctica), Tectonophysics, 626, 69-85.
Biedermann, A. R., C. B. Koch, W. E. A. Lorenz, and A. M. Hirt (2014), Low-temperature magnetic anisotropy in micas and chlorite, Tectonophysics, 629, 63-74.
Biedermann, A. R., T. Pettke, E. Reusser, and A. M. Hirt (2014), Anisotropy of magnetic susceptibility in natural olivine single crystals, Geochemistry Geophysics Geosystems, 15(7), 3051-3065.
Bilardello, D., and M. J. Jackson (2014), A comparative study of magnetic anisotropy measurement techniques in relation to rock-magnetic properties, Tectonophysics, 629, 39-54.
Bolle, O., B. Charlier, J. Bascou, H. Diot, and S. A. McEnroe (2014), Anisotropy of magnetic susceptibility versus lattice- and shape-preferred orientation in the Lac Tio hemo-ilmenite ore body (Grenville province, Quebec), Tectonophysics, 629, 87-108.
Ferre, E. C., A. Gebelin, J. L. Till, C. Sassier, and K. C. Burmeister (2014), Deformation and magnetic fabrics in ductile shear zones: A review, Tectonophysics, 629, 179-188.
Georgiev, N., B. Henry, N. Jordanova, D. Jordanova, and K. Naydenov (2014), Emplacement and fabric-forming conditions of plutons from structural and magnetic fabric analysis: A case study of the Plana pluton (Central Bulgaria), Tectonophysics, 629, 138-154.
Guerrero-Suarez, S., and F. Martin-Hernandez (2014), On the reliability of the AMS ellipsoid by statistical methods, Tectonophysics, 629, 75-86.
Hrouda, F., and J. Jezek (2014), Frequency-dependent AMS of rocks: A tool for the investigation of the fabric of ultrafine magnetic particles, Tectonophysics, 629, 27-38.
Hrouda, F., S. W. Faryad, M. Chlupakova, and P. Jerabek (2014), Magnetic fabric in amphibolized eclogites and serpentinized ultramafites in the Marianske Lazne Complex (Bohemian Massif, Czech Republic): Product of exhumation-driven retrogression?, Tectonophysics, 629, 260-274.
Humbert, F., L. Louis, and P. Robion (2014), Method for estimating ductile horizontal strain from magnetic fabrics in poorly consolidated clay-rich sediments, Tectonophysics, 629, 335-352.
Juan, A. P., et al. (2014), Magnetic fabrics in the Western Central-Pyrenees: An overview, Tectonophysics, 629, 303-318.
Karell, F., C. Ehlers, and M. L. Airo (2014), Emplacement and magnetic fabrics of rapakivi granite intrusions within Wiborg and Aland rapakivi granite batholiths in Finland, Tectonophysics, 614, 31-43.
Kontny, A., and F. Dietze (2014), Magnetic fabrics in deformed metaperidotites of the Outokumpu Deep Drill Core, Finland: Implications for a major crustal shear zone, Tectonophysics, 629, 224-237.
Li, S. H., C. L. Deng, G. A. Paterson, H. T. Yao, S. Huang, C. Y. Liu, H. Y. He, Y. X. Pan, and R. X. Zhu (2014), Tectonic and sedimentary evolution of the late Miocene-Pleistocene Dali Basin in the southeast margin of the Tibetan Plateau: Evidences from anisotropy of magnetic susceptibility and rock magnetic data, Tectonophysics, 629, 362-377.
Lu, H. J., E. Wang, and K. Meng (2014), Paleomagnetism and anisotropy of magnetic susceptibility of the Tertiary Janggalsay section (southeast Tarim basin): Implications for Miocene tectonic evolution of the Altyn Tagh Range, Tectonophysics, 618, 67-78.
Luo, L., J. F. Qi, and M. Z. Zhang (2014), AMS investigation in the Pingluoba and Qiongxi anticlines, Sichuan, China: Implications for deformation mechanism of the Qiongxi structure, Tectonophysics, 626, 186-196.
Machek, M., Z. Rokerova, P. Zavada, P. F. Silva, B. Henry, P. Dedecek, E. Petrovsky, and F. O. Marques (2014), Intrusion of lamprophyre dyke and related deformation effects in the host rock salt: A case study from the Loule diapir, Portugal, Tectonophysics, 629, 165-178.
Mamtani, M. A. (2014), Magnetic fabric as a vorticity gauge in syntectonically deformed granitic rocks, Tectonophysics, 629, 189-196.
Merabet, N. E., Y. Mandjoub, A. Abtout, B. Henry, M. Kahoui, S. Maouche, A. Lamali, and M. Ayache (2014), The Paleoproterozoic Djebel Drissa ring complex (Eglab shield, Algeria): Post-collisional intrusions in a transtentional tectonic setting, Tectonophysics, 629, 197-210.
Mondal, T. K., and M. A. Mamtani (2014), Fabric analysis in rocks of the Gadag region (southern India) - Implications for time relationship between regional deformation and gold mineralization, Tectonophysics, 629, 238-249.
Pares, J. M., and B. A. van der Pluijm (2014), Low-temperature AMS and the quantification of subfabrics in deformed rocks, Tectonophysics, 629, 55-62.
Raposo, M. I. B., C. O. Drukas, and M. A. S. Basei (2014), Deformation in rocks from Itajai basin, Southern Brazil, revealed by magnetic fabrics, Tectonophysics, 629, 290-302.
Robion, P., C. David, J. Dautriat, J. C. Colombier, L. Zinsmeister, and P. Y. Collin (2014), Pore fabric geometry inferred from magnetic and acoustic anisotropies in rocks with various mineralogy, permeability and porosity, Tectonophysics, 629, 109-122.
Schobel, S., and H. de Wall (2014), AMS-NRM interferences in the Deccan basalts: Toward an improved understanding of magnetic fabrics in flood basalts, Journal of Geophysical Research-Solid Earth, 119(4), 2651-2678.
Selkin, P. A., J. S. Gee, and W. P. Meurer (2014), Magnetic anisotropy as a tracer of crystal accumulation and transport, Middle Banded Series, Stillwater Complex, Montana, Tectonophysics, 629, 123-137.
Shimono, T., T. Yamazaki, and S. Inoue (2014), Influence of sampling on magnetic susceptibility anisotropy of soft sediments: comparison between gravity and piston cores, Earth Planets and Space, 66.
Silva, P. F., F. O. Marques, M. Machek, B. Henry, A. M. Hirt, Z. Roxerova, P. Madureira, and S. Vratislav (2014), Evidence for non-coaxiality of ferrimagnetic and paramagnetic fabrics, developed during magma flow and cooling in a thick mafic dyke, Tectonophysics, 629, 155-164.
Soto, R., E. Beamud, B. Oliva-Urcia, E. Roca, M. Rubinat, and J. J. Villalain (2014), Applicability of magnetic fabrics in rocks associated with the emplacement of salt structures (the Bicorb-Quesa and Navarres salt walls, Prebetics, SE Spain), Tectonophysics, 629, 319-334.
Studynka, J., M. Chadima, and P. Suza (2014), Fully automated measurement of anisotropy of magnetic susceptibility using 3D rotator, Tectonophysics, 629, 6-13.
Till, J. L., and B. M. Moskowitz (2014), Deformation microstructures and magnetite texture development in synthetic shear zones, Tectonophysics, 629, 211-223.
Veloso, E. E., N. W. Hayman, R. Anma, M. Tominaga, R. T. Gonzalez, T. Yamazaki, and N. Astudillo (2014), Magma flow directions in the sheeted dike complex at superfast spreading mid-ocean ridges: Insights from IODP Hole 1256D, Eastern Pacific, Geochemistry Geophysics Geosystems, 15(4), 1283-1295.

Mineralogy and Petrology

Alexandrowicz, Z., M. Marszalek, and G. Rzepa (2014), Distribution of secondary minerals in crusts developed on sandstone exposures, Earth Surface Processes and Landforms, 39(3), 320-335.
Biagioni, C., and M. Pasero (2014), The systematics of the spinel-type minerals: An overview, American Mineralogist, 99(7), 1254-1264.
Cao, J., C. Y. Wang, C. M. Xing, and Y. G. Xu (2014), Origin of the early Permian Wajilitag igneous complex and associated Fe-Ti oxide mineralization in the Tarim large igneous province, NW China, Journal of Asian Earth Sciences, 84, 51-68.

Mineral Physics and Chemistry

Adelstein, N., J. B. Neaton, M. Asta, and L. C. De Jonghe (2014), Density functional theory based calculation of small-polaron mobility in hematite, Physical Review B, 89(24).
Baranov, N. V., P. N. G. Ibrahim, N. V. Selezneva, V. A. Kazantsev, A. S. Volegov, and D. A. Shishkin (2014), Crystal structure, phase transitions and magnetic properties of pyrrhotite-type compounds Fe7-xTixS8, Physica B-Condensed Matter, 449, 229-235.
Bhattacharya, S. (2014), Temperature-dependent weak value of dwell time for a two-state particle tunneling through a thermal magnetic barrier, Physical Review A, 89(2).
Bhowmik, R. N., N. Naresh, B. Ghosh, and S. Banerjee (2014), Study of low temperature ferromagnetism, surface paramagnetism and exchange bias effect in alpha-Fe1.4Ga0.6O3 oxide, Current Applied Physics, 14(7), 970-979.
Bosak, A., D. Chernyshov, M. Hoesch, P. Piekarz, M. Le Tacon, M. Krisch, A. Kozlowski, A. M. Oles, and K. Parlinski (2014), Short-Range Correlations in Magnetite above the Verwey Temperature, Physical Review X, 4(1).
Frierdich, A. J., B. L. Beard, M. M. Scherer, and C. M. Johnson (2014), Determination of the Fe(II)(aq)-magnetite equilibrium iron isotope fractionation factor using the three-isotope method and a multi-direction approach to equilibrium, Earth and Planetary Science Letters, 391, 77-86.
Frierdich, A. J., B. L. Beard, T. R. Reddy, M. M. Scherer, and C. M. Johnson (2014), Iron isotope fractionation between aqueous Fe(II) and goethite revisited: New insights based on a multi-direction approach to equilibrium and isotopic exchange rate modification, Geochimica Et Cosmochimica Acta, 139, 383-398.
Kothapalli, K., et al. (2014), Nuclear forward scattering and first-principles studies of the iron oxide phase Fe4O5, Physical Review B, 90(2).
Laha, S. S., R. J. Tackett, and G. Lawes (2014), Interactions in gamma-Fe2O3 and Fe3O4 nanoparticle systems, Physica B-Condensed Matter, 448, 69-72.
Ma, F. X., X. Y. Sun, K. He, J. T. Jiang, L. Zhen, and C. Y. Xu (2014), Hydrothermal synthesis, magnetic and electromagnetic properties of hexagonal Fe3O4 microplates, Journal of Magnetism and Magnetic Materials, 361, 161-165.
Przenioslo, R., I. Sosnowska, M. Stekiel, D. Wardecki, A. Fitch, and J. B. Jasinski (2014), Monoclinic deformation of the crystal lattice of hematite alpha-Fe2O3, Physica B-Condensed Matter, 449, 72-76.

Wen, F. S., F. Zhang, and H. Zheng (2014), Microwave dielectric and magnetic properties of superparamagnetic 8-nm Fe3O4 nanoparticles (vol 324, pg 2471, 2012), Journal of Magnetism and Magnetic Materials, 360, 234-234.

Paleointensity and records of the geomagnetic field

Coe, R. S., N. A. Jarboe, M. Le Goff, and N. Petersen (2014), Demise of the rapid-field-change hypothesis at Steens Mountain: The crucial role of continuous thermal demagnetization, Earth and Planetary Science Letters, 400, 302-312.

de Groot, L. V., M. J. Dekkers, M. Visscher, and G. W. ter Maat (2014), Magnetic properties and paleointensities as function of depth in a Hawaiian lava flow, Geochemistry Geophysics Geosystems, 15(4), 1096-1112.

Dominguez, A. R., and R. Van der Voo (2014), Secular variation of the middle and late Miocene geomagnetic field recorded by the Columbia River Basalt Group in Oregon, Idaho and Washington, USA, Geophysical Journal International, 197(3), 1299-1320.

Eitel, M., S. A. Gilder, T. Kunzmann, and J. Pohl (2014), Rochechouart impact crater melt breccias record no geomagnetic field reversal, Earth and Planetary Science Letters, 387, 97-106.

Ingham, E., D. Heslop, A. P. Roberts, R. Hawkins, and M. Sambridge (2014), Is there a link between geomagnetic reversal frequency and paleointensity? A Bayesian approach, Journal of Geophysical Research-Solid Earth, 119(7), 5290-5304.

Iorio, M., J. Liddicoat, F. Budillon, A. Incoronato, R. S. Coe, D. D. Insinga, W. S. Cassata, C. Lubritto, A. Angelino, and S. Tamburrino (2014), Combined palaeomagnetic secular variation and petrophysical records to time-constrain geological and hazardous events: An example from the eastern Tyrrhenian Sea over the last 120 ka, Global and Planetary Change, 113, 91-109.

Laj, C., H. Guillou, and C. Kissel (2014), Dynamics of the earth magnetic field in the 10-75 kyr period comprising the Laschamp and Mono Lake excursions: New results from the French Chaine des Puys in a global perspective, Earth and Planetary Science Letters, 387, 184-197.

Negrini, R. M., et al. (2014), Nongeocentric axial dipole field behavior during the Mono Lake excursion, Journal of Geophysical Research-Solid Earth, 119(4), 2567-2581.

Oliva-Urcia, B., M. Bartolome, A. Moreno, G. Gil-Romera, C. Sancho, A. Munoz, and M. C. Osakar (2014), Testing the reliability of detrital cave sediments as recorders of paleomagnetic secular variations, Seso Cave System (Central Pyrenees, Spain), Catena, 119, 36-51.

Ouyang, T. P., D. Heslop, A. P. Roberts, C. J. Tian, Z. Y. Zhu, Y. Qiu, and X. C. Peng (2014), Variable remanence acquisition efficiency in sediments containing biogenic and detrital magnetites: Implications for relative paleointensity signal recording, Geochemistry Geophysics Geosystems, 15(7), 2780-2796.

Pena, R. M., A. Goguitchaichvili, M. N. Guilbaud, V. C. R. Martinez, M. C. Rathert, C. Siebe, B. A. Reyes, and J. Morales (2014), Paleomagnetic secular variation study of Ar-Ar dated lavas flows from Tacambaro area (Central Mexico): Possible evidence of Intra-Jaramillo geomagnetic excursion in volcanic rocks, Physics of the Earth and Planetary Interiors, 229, 98-109.

Rolf, C., U. Hambach, A. Novothny, E. Horvath, and E. Schnepp (2014), Dating of a Last Glacial loess sequence by relative geomagnetic palaeointensity: A case study from the Middle Danube Basin (Sutto, Hungary), Quaternary International, 319, 99-108.

Shcherbakova, V. V., V. P. Shcherbakov, G. V. Zhidkov, and N. V. Lubnina (2014), Palaeointensity determinations on rocks from Palaeoproterozoic dykes from the Kaapvaal Craton (South Africa), Geophysical Journal International, 197(3), 1371-1381.

Singer, B. S. (2014), A Quaternary geomagnetic instability time scale, Quaternary Geochronology, 21, 29-52.

Singer, B. S., H. Guillou, B. R. Jicha, E. Zanella, and P. Camps (2014), Refining the Quaternary Geomagnetic Instability Time Scale (GITS): Lava flow recordings of the Blake and Post-Blake excursions, Quaternary Geochronology, 21, 16-28.

Suavet, C., B. P. Weiss, and T. L. Grove (2014), Controlled-atmosphere thermal demagnetization and paleointensity analyses of extraterrestrial rocks, Geochemistry Geophysics Geosystems, 15(7), 2733-2743.

Veikkolainen, T., L. Pesonen, and K. Korhonen (2014), An analysis of geomagnetic field reversals supports the validity of the Geocentric Axial Dipole (GAD) hypothesis in the Precambrian, Precambrian Research, 244, 33-41.

Veikkolainen, T., D. A. D. Evans, K. Korhonen, and L. J. Pesonen (2014), On the low-inclination bias of the Precambrian geomagnetic field, Precambrian Research, 244, 23-32.

Zhao, X. Y., Q. S. Liu, G. A. Paterson, H. F. Qin, S. H. Cai, Y. Yu, and R. X. Zhu (2014), The effects of secondary mineral formation on Coe-type paleointensity determinations: Theory and simulation, Geochemistry Geophysics Geosystems, 15(4), 1215-1234.

Paleomagnetism

Advokaat, E. L., D. J. J. van Hinsbergen, M. Maffione, C. G. Langereis, R. L. M. Vissers, A. Cherchi, R. Schroeder, H. Madani, and S. Columbu (2014), Eocene rotation of Sardinia, and the paleogeography of the western Mediterranean region, Earth and Planetary Science Letters, 401, 183-195.

Aubele, K., V. Bachtadse, G. Muttoni, and A. Ronchi (2014), Paleomagnetic data from Late Paleozoic dykes of Sardinia: Evidence for block rotations and implications for the intra-Pangea megashear system, Geochemistry Geophysics Geosystems, 15(5), 1684-1697.

Belica, M. E., E. J. Piispa, J. G. Meert, L. J. Pesonen, J. Plado, M. K. Pandit, G. D. Kamenov, and M. Celestino (2014), Paleoproterozoic mafic dyke swarms from the Dharwar craton; paleomagnetic poles for India from 2.37 to 1.88 Ga and rethinking the Columbia supercontinent, Precambrian Research, 244, 100-122.

Bispo-Santos, F., M. S. D'Agrella, R. I. F. Trindade, L. Janikian, and N. J. Reis (2014), Was there SAMBA in Columbia? Paleomagnetic evidence from 1790 Ma Avanavero mafic sills (northern Amazonian Craton), Precambrian Research, 244, 139-155.

Bispo-Santos, F., M. S. D'Agrella, L. Janikian, N. J. Reis, R. I. F. Trindade, and M. Reis (2014), Towards Columbia: Paleomagnetism of 1980-1960 Ma Surumu volcanic rocks, Northern Amazonian Craton, Precambrian Research, 244, 123-138.

Bottrill, A. D., J. van Hunen, S. J. Cuthbert, H. K. Brueckner, and M. B. Allen (2014), Plate rotation during continental collision and its relationship with the exhumation of UHP metamorphic terranes: Application to the Norwegian Caledonides, Geochemistry Geophysics Geosystems, 15(5), 1766-1782.

Buchan, K. L. (2014), Reprint of "Key paleomagnetic poles and their use in Proterozoic continent and supercontinent reconstructions: A review", Precambrian Research, 244, 5-22.

Caccavari, A., M. Calvo-Rathert, A. Goguitchaichvili, H. Y. He, G. Vashakidze, and N. Vegas (2014), Palaeomagnetism and Ar-40/Ar-39 age of a Pliocene lava flow sequence in the Lesser Caucasus: record of a clockwise rotation and analysis of palaeosecular variation, Geophysical Journal International, 197(3), 1354-1370.

Caricchi, C., F. Cifelli, L. Sagnotti, F. Sani, F. Speranza, and M. Mattei (2014), Paleomagnetic evidence for a post-Eocene 90 degrees CCW rotation of internal Apennine units: A linkage with Corsica-Sardinia rotation?, Tectonics, 33(4), 374-392.

Davis, J. K., J. G. Meert, and M. K. Pandit (2014), Paleomagnetic analysis of the Marwar Supergroup, Rajasthan, India and proposed interbasinal correlations, Journal of Asian Earth Sciences, 91, 339-351.

de Groot, L. V., K. Fabian, I. A. Bakelaar, and M. J. Dekkers (2014), Magnetic force microscopy reveals meta-stable magnetic domain states that prevent reliable absolute palaeointensity experiments, Nature Communications, 5.

Du, L. L., J. H. Guo, A. P. Nutman, D. Wyman, Y. S. Geng, C. H. Yang, F. L. Liu, L. D. Ren, and X. W. Zhou (2014), Implications for Rodinia reconstructions for the initiation of Neoproterozoic subduction at similar to 860 Ma on the western margin of the Yangtze Block: Evidence from the Guandaoshan Pluton, Lithos, 196, 67-82.

Dunlop, D. J. (2014), Grenvillia and Laurentia - a Precambrian Wilson cycle?, Canadian Journal of Earth Sciences, 51(3), 187-196.

Elming, S. A., S. A. Pisarevsky, P. Layer, and G. Bylund (2014), A palaeomagnetic and Ar-40/Ar-39 study of mafic dykes in southern Sweden: A new Early Neoproterozoic key-pole for the Baltic Shield and implications for Sveconorwegian and Grenville loops, Precambrian Research, 244, 192-206.

Ferre, E. C., S. A. Friedman, F. Martin-Hernandez, J. M. Feinberg, J. L. Till, D. A. Ionov, and J. A. Conder (2014), Eight good reasons why the uppermost mantle could be magnetic, Tectonophysics, 624, 3-14.

Halls, H. (2014), Crustal shortening during the Paleoproterozoic: Can it be accommodated by paleomagnetic data?, Precambrian Research, 244, 42-52.

Heslop, D., A. P. Roberts, and R. Hawkins (2014), A statistical simulation of magnetic particle alignment in sediments, Geophysical Journal International, 197(2), 828-837.

Hirt, A. M., A. R. Biedermann, and N. S. Mancktelow (2014), Magnetic study of a late Alpine dike crosscutting the regional foliation, Tectonophysics, 629, 250-259.

Hnatyshin, D., and V. A. Kravchinsky (2014), Paleomagnetic dating: Methods, MATLAB software, example, Tectonophysics, 630, 103-112.

Hoffman, P. F. (2014), Tuzo Wilson and the acceptance of pre-Mesozoic continental drift, Canadian Journal of Earth Sciences, 51(3), 197-207.

Keppie, D. F., and J. D. Keppie (2014), The Yucatan, a Laurentian or Gondwanan fragment? Geophysical and palinspastic constraints, International Journal of Earth Sciences, 103(5), 1501-1512.

Klein, R., L. J. Pesonen, J. Salminen, and S. Mertanen (2014), Paleomagnetism of Mesoproterozoic Satakunta sandstone, Western Finland, Precambrian Research, 244, 156-169.

Kornfeld, D., S. Eckert, E. Appel, L. Ratschbacher, J. Pfander, D. L. Liu, and L. Ding (2014), Clockwise rotation of the Baoshan Block due to southeastward tectonic escape of Tibetan crust since the Oligocene, Geophysical Journal International, 197(1), 149-163.

Kornfeld, D., S. Eckert, E. Appel, L. Ratschbacher, B. L. Sonntag, J. A. Pfander, L. Ding, and D. L. Liu (2014), Cenozoic clockwise rotation of the Tengchong block, southeastern Tibetan Plateau: A paleomagnetic and geochronologic study, Tectonophysics, 628, 105-122.

Lubnina, N. V., S. A. Pisarevsky, V. N. Puchkov, V. I. Kozlov, and N. D. Sergeeva (2014), New paleomagnetic data from Late Neoproterozoic sedimentary successions in Southern Urals, Russia: implications for the Late Neoproterozoic paleogeography of the Iapetan realm, International Journal of Earth Sciences, 103(5), 1317-1334.

Marton, E., V. Cosovic, and A. Moro (2014), New stepping stones, Dugi otok and Vis islands, in the systematic paleomagnetic study of the Adriatic region and their significance in evaluations of existing tectonic models, Tectonophysics, 611, 141-154.

Mochales, T., and T. G. Blenkinsop (2014), Representation of paleomagnetic data in virtual globes: A case study from the Pyrenees, Computers & Geosciences, 70, 56-62.

Petronis, M. S., D. K. Holm, J. W. Geissman, D. B. Hacker, and B. J. Arnold (2014), Paleomagnetic results from the eastern Caliente-Enterprise zone, southwestern Utah: Implications for initiation of a major Miocene transfer zone, Geosphere, 10(3), 534-563.

Pisarevsky, S. A., S. A. Elming, L. J. Pesonen, and Z. X. Li (2014), Mesoproterozoic paleogeography: Supercontinent and beyond, Precambrian Research, 244, 207-225.

Pisarevsky, S. A., M. T. D. Wingate, Z. X. Li, X. C. Wang, E. Tohver, and C. L. Kirkland (2014), Age and paleomagnetism of the 1210 Ma Gnowangerup-Fraser dyke swarm, Western Australia, and implications for late Mesoproterozoic paleogeography, Precambrian Research, 246, 1-15.

Salminen, J., S. Mertanen, D. A. D. Evans, and Z. Wang (2014), Paleomagnetic and geochemical studies of the Mesoproterozoic Satakunta dyke swarms, Finland, with implications for a Northern Europe - North America (NENA) connection within Nuna supercontinent, Precambrian Research, 244, 170-191.

Salminen, J., H. C. Halls, S. Mertanen, L. J. Pesonen, J. Vuollo, and U. Soderlund (2014), Paleomagnetic and geochronological studies on Paleoproterozoic diabase dykes of Karelia, East Finland-Key for testing the Superia supercraton, Precambrian Research, 244, 87-99.

Schmidt, P. W. (2014), A review of Precambrian palaeomagnetism of Australia: Palaeogeography, supercontinents, glaciations and true polar wander, Gondwana Research, 25(3), 1164-1185.

Shao, Q. F., W. Wang, C. L. Deng, P. Voinchet, M. Lin, A. Zazzo, E. Douville, J. M. Dolo, C. Falgueres, and J. J. Bahain (2014), ESR, U-series and paleomagnetic dating of Gigantopithecus fauna from Chuifeng Cave, Guangxi, southern China, Quaternary Research, 82(1), 270-280.

Sonnette, L., F. Humbert, C. Aubourg, J. Gattacceca, J. C. Lee, and J. Angelier (2014), Significant rotations related to cover-substratum decoupling: Example of the Dome de Barrot (Southwestern Alps, France), Tectonophysics, 629, 275-289.

Suttie, N., A. J. Biggin, and R. Holme (2014), Correlation of palaeomagnetic directions constrains eruption rate of large igneous provinces, Earth and Planetary Science Letters, 387, 4-9.

Swanson-Hysell, N. L., A. A. Vaughan, M. R. Mustain, and K. E. Asp (2014), Confirmation of progressive plate motion during the Midcontinent Rift's early magmatic stage from the Osler Volcanic Group, Ontario, Canada, Geochemistry Geophysics Geosystems, 15(5), 2039-2047.

Torsvik, T. H., R. van der Voo, P. V. Doubrovine, K. Burke, B. Steinberger, L. D. Ashwal, R. G. Tronnes, S. J. Webb, and A. L. Bull (2014), Deep mantle structure as a reference frame for movements in and on the Earth, Proceedings of the National Academy of Sciences of the United States of America, 111(24), 8735-8740.

Wang, E., K. Meng, Z. Su, Q. R. Meng, J. J. Chu, Z. L. Chen, G. Wang, X. H. Shi, and X. Q. Liang (2014), Block rotation: Tectonic response of the Sichuan basin to the southeastward growth of the Tibetan Plateau along the Xianshuihe-Xiaojiang fault, Tectonics, 33(5), 686-717.

Wei, W., Y. Chen, M. Faure, Y. H. Shi, G. Martelet, Q. L. Hou, W. Lin, N. Le Breton, and Q. C. Wang (2014), A multidisciplinary study on the emplacement mechanism of the Qingyang-Jiuhua Massif in Southeast China and its tectonic b Part I: Structural geology, AMS and paleomagnetism, Journal of Asian Earth Sciences, 86, 76-93.

Wu, L., and V. A. Kravchinsky (2014), Derivation of paleolongitude from the geometric parametrization of apparent polar wander path: Implication for absolute plate motion reconstruction, Geophysical Research Letters, 41(13), 4503-4511.

Xu, J. Y., Z. Ben-Avraham, T. Kelty, and H. S. Yu (2014), Origin of marginal basins of the NW Pacific and their plate tectonic reconstructions, Earth-Science Reviews, 130, 154-196.

Zhao, P., Y. Chen, S. Zhan, B. Xu, and M. Faure (2014), The Apparent Polar Wander Path of the Tarim block (NW China) since the Neoproterozoic and its implications for a long-term Tarim-Australia connection, Precambrian Research, 242, 39-57.

Spectroscopy and Imaging

Ludwig, F., H. Remmer, C. Kuhlmann, T. Wawrzik, H. Arami, R. M. Ferguson, and K. M. Krishnan (2014), Self-consistent magnetic properties of magnetite tracers optimized for magnetic particle imaging measured by ac susceptometry, magnetorelaxometry and magnetic particle spectroscopy, Journal of Magnetism and Magnetic Materials, 360, 169-173.

Sobron, P., J. L. Bishop, D. F. Blake, B. Chen, and F. Rull (2014), Natural Fe-bearing oxides and sulfates from the Rio Tinto Mars analog site: Critical assessment of VNIR reflectance spectroscopy, laser Raman spectroscopy, and XRD as mineral identification tools, American Mineralogist, 99(7), 1199-1205.

Stratigraphy

Baksi, A. K. (2014), The Deccan Trap - Cretaceous-Paleogene boundary connection; new Ar-40/Ar-39 ages and critical assessment of existing argon data pertinent to this hypothesis, Journal of Asian Earth Sciences, 84, 9-23.

Opdyke, N. D., P. S. Giles, and J. Utting (2014), Magnetic polarity stratigraphy and palynostratigraphy of the Mississippian-Pennsylvanian boundary interval in eastern North America and the age of the beginning of the Kiaman, Geological Society of America Bulletin, 126(7-8), 1068-1083.

Wack, M. R., S. A. Gilder, E. A. Macaulay, E. R. Sobel, J. Charreau, and A. Mikolaichuk (2014), Cenozoic magnetostratigraphy and magnetic properties of the southern Issyk-Kul basin, Kyrgyzstan, Tectonophysics, 629, 14-26.

Zhang, T., X. M. Fang, C. H. Song, E. Appel, and Y. D. Wang (2014), Cenozoic tectonic deformation and uplift of the South Tian Shan: Implications from magnetostratigraphy and balanced cross-section restoration of the Kuqa depression, Tectonophysics, 628, 172-187.

Zhang, W. L., E. Appel, X. M. Fang, C. H. Song, F. Setzer, C. Herb, and M. D. Yan (2014), Magnetostratigraphy of drill-core SG-1b in the western Qaidam Basin (NE Tibetan Plateau) and tectonic implications, Geophysical Journal International, 197(1), 90-118.

Surveying

Adetunji, A. Q., I. J. Ferguson, and A. G. Jones (2014), Crustal and lithospheric scale structures of the Precambrian Superior-Grenville margin, Tectonophysics, 614, 146-169.

Bedrosian, P. A., and D. W. Feucht (2014), Structure and tectonics of the northwestern United States from Earth Scope USArray magnetotelluric data, Earth and Planetary Science Letters, 402, 275-289.

Bouligand, C., J. M. G. Glen, and R. J. Blakely (2014), Distribution of buried hydrothermal alteration deduced from high-resolution magnetic surveys in Yellowstone National Park, Journal of Geophysical Research-Solid Earth, 119(4), 2595-2630.

Carvalho, J., T. Rabeh, R. Dias, C. Pinto, T. Oliveira, T. Cunha, and J. Borges (2014), Tectonic and neotectonic implications of a new basement map of the Lower Tagus Valley, Portugal, Tectonophysics, 617, 88-100.

Cherevatova, M., M. Smirnov, T. Korja, P. Kaikkonen, L. B. Pedersen, J. Hubert, J. Kamm, and T. Kalscheuer (2014), Crustal structure beneath southern Norway imaged by magnetotellurics, Tectonophysics, 628, 55-70.

Elkhodary, S., and T. Rabeh (2014), Role of Lithology and Subsurface structures detected by potential field data in controlling the radioactive mineral accumulation at Natash area, Eastern Desert, Egypt, Geofisica Internacional, 53(3), 309-319.

Garcia-Lobon, J. L., C. Rey-Moral, C. Ayala, L. M. Martin-Parra, J. Matas, and M. I. Reguera (2014), Regional structure of the southern segment of Central Iberian Zone (Spanish Variscan Belt) interpreted from potential field images and 2.5 D modelling of Alcudia gravity transect, Tectonophysics, 614, 185-202.

Hanan, G., R. Michael, S. Boris, and L. Michael (2014), Magmatic occurrences in the Central Arava (southern Israel) based on Geology and Magnetometry, Journal of Asian Earth Sciences, 85, 106-116.

Mieth, M., J. Jacobs, A. Ruppel, D. Damaske, A. Laufer, and W. Jokat (2014), New detailed aeromagnetic and geological data of eastern Dronning Maud Land: Implications for refining the tectonic and structural framework of Sor Rondane, East Antarctica, Precambrian Research, 245, 174-185.

Obande, G. E., K. M. Lawal, and L. A. Ahmed (2014), Spectral analysis of aeromagnetic data for geothermal investigation of Wikki Warm Spring, northeast Nigeria, Geothermics, 50, 85-90.

Sato, T., H. Oda, O. Ishizuka, and K. Arai (2014), Detailed bathymetry and magnetic anomaly in the Central Ryukyu Arc, Japan: implications for a westward shift of the volcanic front after approximately 2.1 Ma, Earth Planets and Space, 66.

Stein, C. A., S. Stein, M. Merino, G. R. Keller, L. M. Flesch, and D. M. Jurdy (2014), Was the Midcontinent Rift part of a successful seafloor- spreading episode?, Geophysical Research Letters, 41(5), 1465-1470.

Other

Debret, B., M. Andreani, M. Munoz, N. Bolfan-Casanova, J. Carlut, C. Nicollet, S. Schwartz, and N. Trcera (2014), Evolution of Fe redox state in serpentine during subduction, Earth and Planetary Science Letters, 400, 206-218.

Dologlou, E. (2014), A physical model for the precursory magnetic anomalies of the M5.4 Alum Rock and M6.0 Parkfield earthquakes, International Journal of Earth Sciences, 103(4), 977-980.

Enkin, R. J. (2014), The Rock Physical Property Database of British Columbia, and the distinct petrophysical signature of the Chilcotin basalts, Canadian Journal of Earth Sciences, 51(4), 327-338.

Jiang, F. Y., X. Y. Li, Y. Zhu, and Z. K. Tang (2014), Synthesis and magnetic characterizations of uniform iron oxide nanoparticles, Physica B-Condensed Matter, 443, 1-5.

Wallis, D., A. J. Parsons, R. J. Phillips, M. P. Searle, and E. C. Ferre (2014), Comment on "Interplay of deformation and magmatism in the Pangong Transpressional Zone, Eastern Ladakh, India: Implications for remobilization of the trans-Himalayan magmatic arc and initiation of the Karakoram Fault" by K. Sen, BK Mukherjee and AS Collins, Journal of Structural Geology 62 (2014) 13-24, Journal of Structural Geology, 65, 117-119.

cont'd. from pg. 1...

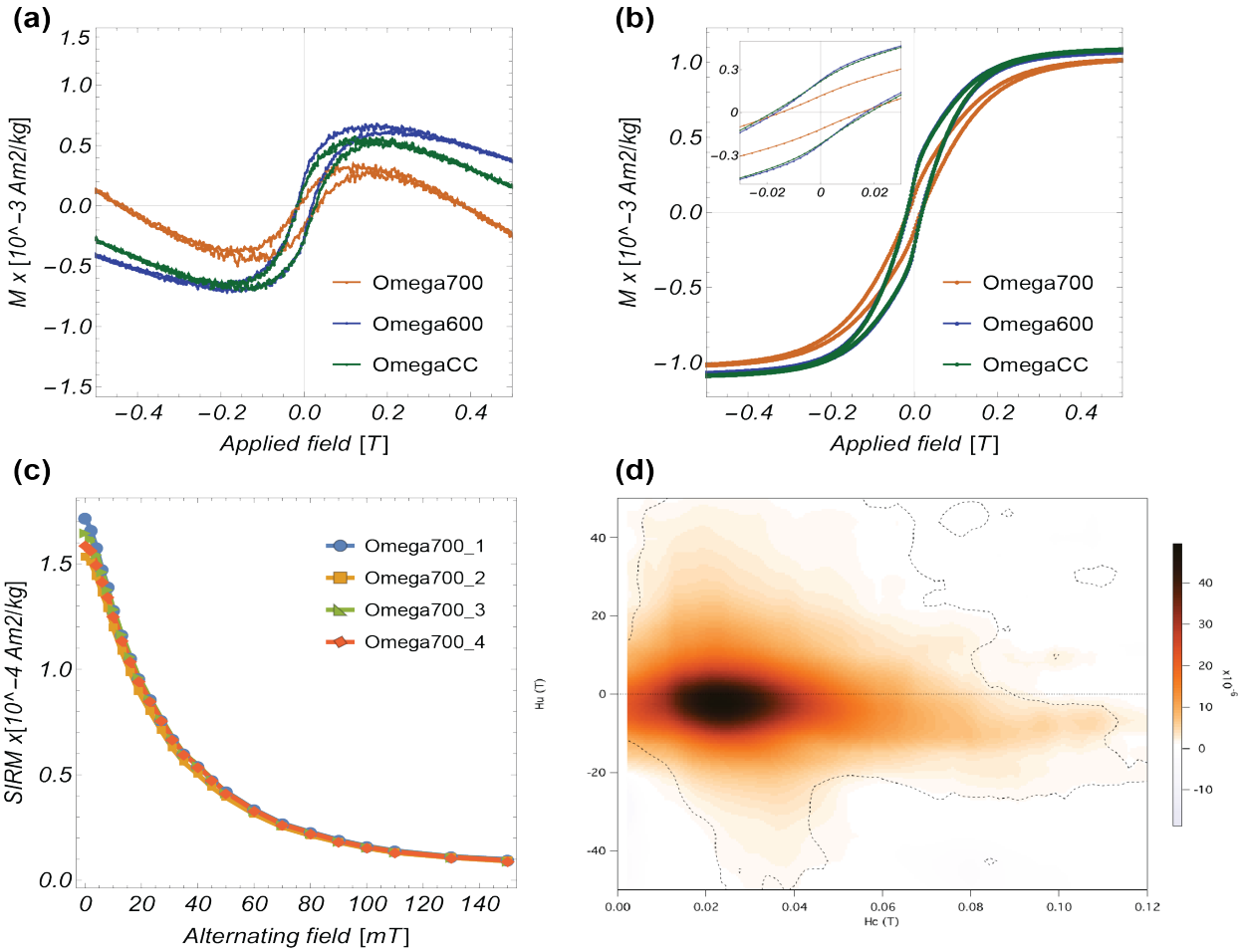

Fig 2. Raw data (a) and filtered data (b) of hysteresis loops of samples Omega 700_7, Omega600, OmegaCC; (c) Stepwise AF demagnetization of SIRM of four samples of Omega700. SIRM was imparted at RT using a field of 1 T; (d) First-order reversal curve (FORC) diagram for sample Omega700_test3, produced using FORCinel (Harrison & Feinberg, 2008) with the VARIFORC smoothing method (Sc0=Sb0=5.5, Sc1=Sb1=8; lambda=0.1). The dashed lines indicate the limits of statistically significant signal.

to +1400°C), moderately heat conductive, resistant to most acids, electrically insulative, and they adhere to virtually any surface. This study examines the magnetic properties of three different cements from Omega Engineering Inc.: Omegabond® 600 Chemical Set Cement ("OB-600"), Omegabond® 700 Chemical Set Cement ("OB-700"), and CC High Temperature Cement ("Omega CC").

OB-600 is made primarily out of zirconium silicate ($ZrSiO_4$) with lesser amounts of magnesium oxide (MgO), and magnesium phosphate ($Mg(H_2PO_4)_2 \cdot H_2O$). When water is added to the cement, an acid-base reaction occurs between the MgO and the phosphate, resulting in the formation of a gel that ultimately crystallizes into an insoluble phosphate mineral. The zirconium silicate acts as an inert filler that is cemented in place by the newly crystallized phosphate. This cement is stable to 1427°C.

OB-700 is made primarily out of quartz (SiO_2) with lesser amounts of sodium disilicate ($Na_2O \cdot (SiO_2)_2$), sodium fluorosilicate (Na_2SiF_6), and magnesium aluminum silicate (clay). Sodium disilicate is also known as "waterglass" or "liquid glass" and is frequently used as binder to help stabilize archaeological materials. Waterglass is produced by mixing natural quartz sand in a steam reactor with sodium hydroxide (NaOH) to form the reaction:

$$2\ SiO_2 + 2\ NaOH \rightarrow Na_2O \cdot (SiO_2)_2 + H_2O$$

Awareness of this production technique is important for magnetic studies because it can include trace amounts of iron, which frequently occurs within natural quartz sands as pigmentary hematite coatings or as Fe-bearing mineral inclusions. Such iron is typically converted to goethite (α-FeO·OH) during the production of dried sodium disilicate. When water is added to OB-700, the Na_2SiF_6 acidifies the $Na_2O \cdot (SiO_2)_2$ allowing the silicon dioxide groups to polymerize, while the quartz and clay act as inert fillers. The quartz and clay are also likely to contain trace concentrations of Fe-bearing materials. This cement is stable to 827°C.

Omega CC is a two-part cement consisting of a powder filler composed of $ZrSiO_4$ and Na_2SiF_6 as well as a liquid binder composed of waterglass mixed with water. When the powder and binder are mixed, the same chemical reaction that describes the setting of OB-700 occurs within the Omega CC cement. The $ZrSiO_4$ again acts as

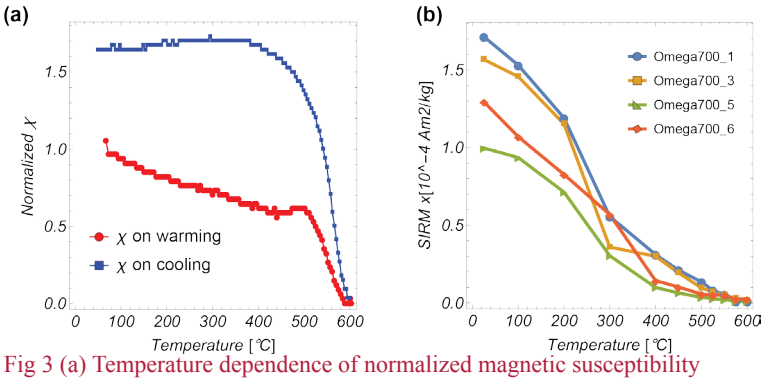

Fig 3 (a) Temperature dependence of normalized magnetic susceptibility from 50°C to 600°C to 50°C in argon for sample Omega700_4; (b) Thermal demagnetization curves of SIRM of four samples of Omega 700. SIRM was imparted at room temperature using a field of 1 T. Samples were thermally demagnetized in air.

an inert filler material that also happens to be resistant to acid corrosion. This cement is stable to 843°C.

Results

Each cement sample in this study was prepared as a 5 mm diameter cylinder that was 10 mm tall and was mixed according to the directions provided by Omega Engineering, Inc. (OB-700: mixture of 25% water to 75% powder by weight; OB-600: mixture of 13 parts water to 100 parts powder by weight; Omega CC: mixture of 20% liquid binder to 80% powder filler by weight). All samples cured in the air at room temperature for 24 hours.

Low-temperature measurements were performed using Quantum Designs MPMS instruments cycling between 300 K and 20 K. Hysteresis loops and first order reversal curve (FORC) experiments were carried out on a Princeton Measurements VSM. Multiple FORC measurements (2-5) were collected for each sample and then averaged to improve the resolution of the resulting coercivity distributions. Samples were demagnetized using stepwise thermal treatments in air to a maximum temperature of 600°C. Isothermal remanent magnetization was measured after each temperature step using 2G Magnetometer. The same magnetometer was also used for alternating field (AF) demagnetization experiments. Room temperature (RT) magnetic susceptibility measurements were conducted on a Kappabridge KLY-2. The temperature dependence of magnetic susceptibility was measured using a MFK1 Kappabridge and CS4 oven across a temperature range from 50°C to 600°C in argon using a 350 Am^{-1} field.

Low Temperature Measurements

Low temperature measurements of typical samples of the three unheated cements are shown in Figure 1. All samples exhibit a Verwey transition at 120 K, indicating the presence of stoichiometric magnetite. In addition, the presence of goethite in OB-700 and OB-600 samples is indicated by a continuous increase of RT SIRM with decreasing temperature and a separation of ZFC and FC curves persisting to 300 K.[1] Evidence of goethite in the Omega CC sample is negligible, suggesting that the liquid form of sodium disilicate in the binder contains less of the iron hydroxide than the powdered form.

Room Temperature Measurements

All samples showed extremely low values of mass normalized susceptibility on the order of 10-9 m^3kg^{-1} (Table 1), which can be explained as the superposition of diamagnetic materials with trace amount of ferrimagnetic material.

All samples displayed hysteresis loops with negative (diamagnetic) high-field slopes and hysteresis parameters typical for pseudo-single domain (PSD) particles of magnetite[2]. Representative hysteresis loops for each type of cement are shown in Figure 2a and 2b. Average ratios of Mrs/Ms and Hcr/Hc for OB-700 samples are 0.12 and 4, respectively, whereas samples of other two types of cements exhibited greater Mrs/Ms ratios – 0.2 and 0.23 and lower Hcr/Hc ratios – 0.2 and 2.5 for OB-600 and Omega CC, respectively (See Table 1). Hysteresis loops of all samples reached approximately the same mass normalized saturation Ms ~$1.1x10^{-3}$ Am^2kg^{-1}. It is also worth noting that the magnetic properties of OB-700 are quite homogeneous among all 7 samples, as indicated by their hysteresis parameters, which are distributed with standard deviations not exceeding 15% of their mean.

FORC diagrams performed on 3 samples of Omega700 displayed median Hc values of ~20 mT which agrees well with the average bulk coercivity value of 15 mT and is again suggestive of PSD magnetite[3] (Figure 2d). Although the sample strength was quite weak, the FORC distribution in Figure 2d also shows a population of non-interacting single domain grains with coercivities up to ~80 mT.

Along these lines, stepwise AF demagnetization of a 1T SIRM for 4 samples of OB-700 exhibited a median destructive field (MDF) of ~25 mT, typical for PSD magnetite (Figure 2c); broadly consistent with the hysteresis and FORC data. The maximum AF of 150 mT was unable to remove ~10% of the SIRM, suggesting that goethite and/or ultrafine single domain magnetite are responsible for this higher coercivity component[4].

High Temperature Measurements

High temperature (HT) experiments were conducted only on OB-700 samples. HT susceptibility dependence measured on sample Omega700_4 (Figure 3a) indicated a Curie temperature of 590°C, suggestive of partially oxidized magnetite (maghemite). RT susceptibility increased by ~60% after heating the sample up to 600°C in argon, evidence of the growth of new magnetic material.

Thermal demagnetization of 1T SIRM performed on 4 samples of OB-700 showed a distributed range of unblocking temperatures (T_{ub}) with the highest T_{ub} at 580°C, the Curie temperature for pure magnetite (Figure 3b). Interestingly, 80-90% of remanence was destroyed below 400°C, which we interpret as evidence of partially oxidized magnetite.

Changes in low-temperature and hysteresis properties of Omega700 samples after high temperature treatments in air or argon are presented in Figure 4. All samples heated in air displayed significantly smaller Ms

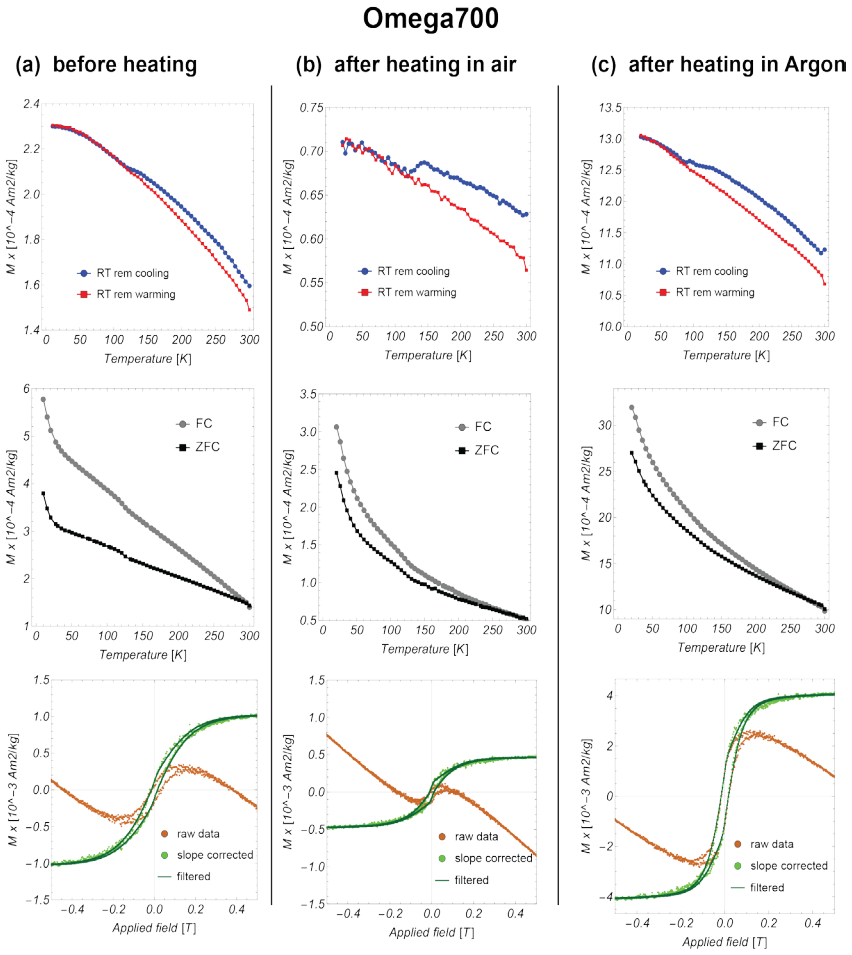

Fig 4. RT SIRM curves on cooling from 300 K to 10 K and warming from 10 K to 300 K (top pictures), SIRM warming curves from 10 K to 300 K after FC and ZFC (central pictures), and hysteresis loops at RT (bottom pictures) of samples (a) Omega700_4 before heating, (b) Omega700_3 after heating up to 600°C in air, and (c) Omega700_4 after heating up to 600°C in argon.

values, decreasing more than 50%. (Figure 4b). This drop in SIRM can be caused by continued oxidation of maghemite to hematite in air[4]. On the other hand, heating in argon produced a near four-fold increase in Ms to ~4 x 10^{-3} Am^2kg^{-1} (Figure 4c). This rise in saturation magnetization indicates the production of new magnetic material during heating, likely magnetite or maghemite from a goethite precursor.

Concluding thoughts and ways forward

Even though Omega cements are commonly thought to be purely diamagnetic, all the samples examined here displayed the presence of magnetite (or its partially oxidized equivalent) and two of the three cements also contained magnetically detectable goethite. The typical Ms for the unheated cements rivals the mass normalized saturation magnetization of a variety of natural sediments (e.g., pelagic limestones, argillaceous rocks, some sandstones, etc.). Heating of OB-700 to high temperatures in air decreased the room temperature saturation magnetization by ~50%, while heating in argon increased room temperature Ms by ~400%. Thus, the use of Omega cements with magnetically weak materials may be problematic because of magnetic contamination and possible misinterpretation of thermomagnetic data.

It may be possible for rock and paleomagnetic labs to reduce the concentration of magnetic contamination in Omega cements, for example, by sending the powder through a very clean Franz magnetic separator multiple times. Chemical treatments to remove magnetite or goethite are unlikely to be successful, as the acids that are typically used to dissolve iron oxides and oxhydroxides would also alter the Na_2SiF_6 and $Na_2O{\cdot}(SiO_2)_2$. We've contacted Omega Engineering Inc. regarding the iron concentrations in their cements and their technical staff are currently exploring whether it would be possible to produce a high purity, high temperature cement specifically for rock magnetic and paleomagnetic applications.

Regardless, Omega high temperature cements continue to be an important tool for high temperature rock magnetic measurements. For most geologic materials the background magnetization of the cement will be insignificant. Additionally, the volume of cement used in most rock magnetic applications, and hence its ability to contaminate a magnetic measurement is relatively small. However, if your materials are weakly magnetic, then the issue of iron contamination in cement may remain, well, incurable.

References

[1]Dekkers, M.J. Magnetic properties of natural goethite-II. TRM behaviour during thermal and alternating field demagnetization and low-temperature treatment(1989) Geophysical Journal, 97 (2), pp. 341-355.

[2]Dunlop, D.J. Theory and application of the Day plot (Mrs/Ms versus Hcr/Hc) 1. Theoretical curves and tests using titanomagnetite data (2002) Journal of Geophysical Research: Solid Earth, 107 (3), pp. 4-1 - 4-22.

[3]Roberts, A.P., Pike, C.R., Verosub, K.L.First-order reversal curve diagrams: A new tool for characterizing the magnetic properties of natural samples (2000) Journal of Geophysical Research: Solid Earth, 105 (B12), art. no. 2000JB900326, pp. 28461-28475.

[4]Dunlop, D. J., and Ö. Özdemir, Rock Magnetism: Fundamentals and Frontiers, 573 pp., Cambridge Univ. Press, New York, 1997.

Sample	χ (10^{-9} m^3/kg)	M_s (10^{-3} Am^2/kg)	M_{rs} (10^{-3} Am^2/kg)	M_{rs} /M_s	H_c (mT)	H_{cr} (mT)	H_{cr} /H_c
Omega700_1	4	1.2	0.12	0.10	10		
Omega700_2	3	1.1	0.14	0.13	18		
Omega700_3	5	1.2	0.12	0.10	12	50	4.3
Omega700_4	1	1.0	0.16	0.16	21		
Omega700_5	2		0.10			60	
Omega700_6	0		0.13				
Omega700_7	-2	1.0	0.12	0.12	15	55	3.7
Omega700_Ave	2	1.1	0.13	0.12	15	55	4.0
St Dev	2	0.1	0.02	0.02	5	5	0.3
Omega600	11	1.1	0.26	0.23	17	43	2.6
OmegaCC	6	1.1	0.23	0.20	18	38	2.1

Table 1. Magnetic Susceptibility and Hysteresis Parameters

University of Minnesota
291 Shepherd Laboratories
100 Union Street S. E.
Minneapolis, MN 55455-0128
phone: (612) 624-5274
fax: (612) 625-7502
e-mail: irm@umn.edu
www.irm.umn.edu

Nonprofit Org.
U.S Postage
PAID
Twin Cities, MN
Permit No. 90155

The IRM Quarterly

The *Institute for Rock Magnetism* is dedicated to providing state-of-the-art facilities and technical expertise free of charge to any interested researcher who applies and is accepted as a Visiting Fellow. Short proposals are accepted semi-annually in spring and fall for work to be done in a 10-day period during the following half year. Shorter, less formal visits are arranged on an individual basis through the Facilities Manager.

The *IRM* staff consists of **Subir Banerjee**, Professor/Founding Director; **Bruce Moskowitz**, Professor/Director; **Joshua Feinberg**, Assistant Professor/Associate Director; **Mike Jackson, Peat Sølheid** and **Dario Bilardello**, Staff Scientists.

Funding for the *IRM* is provided by the **National Science Foundation**, the **W. M. Keck Foundation**, and the **University of Minnesota**.

The *IRM Quarterly* is published four times a year by the staff of the *IRM*. If you or someone you know would like to be on our mailing list, if you have something you would like to contribute (*e.g.*, titles plus abstracts of papers in press), or if you have any suggestions to improve the newsletter, please notify the editor:

Dario Bilardello
Institute for Rock Magnetism
University of Minnesota
291 Shepherd Laboratories
100 Union Street S. E.
Minneapolis, MN 55455-0128
phone: (612) 624-5274
fax: (612) 625-7502
e-mail: dario@umn.edu
www.irm.umn.edu

UNIVERSITY OF MINNESOTA